Cryopreservation of cerebrospinal fluid cells preserves transcriptomics integrity for single-cell analysis

Mahesh Kodali Ph.D.[1,2,¶,*], Jerry Antone Ph.D.[3,¶], Eric Alsop Ph.D.[3], Rojashree Jayakumar M.S.[1], Khushi Parikh B.S.[3], Paula Sanchez-Molina Ph.D.[4], Bahareh Ajami Ph.D.[4], Steven Arnold MD[1,2], Kendall Jensen[3,&], Sudeshna Das Ph.D.[1,2,&], Marc S. Weinberg MD Ph.D.[1,2,5,&,*]

[1] Department of Neurology, Massachusetts General Hospital, Boston, MA, United States of America

[2] Harvard Medical School, Boston, MA, United States of America

[3] Neurogenomics Division, Translational Genomics Research Institute, Phoenix, AZ, United States of America

[4] Department of Molecular Microbiology and Immunology, Oregon Health and Science University, Portland, OR, United States of America

[5] Department of Psychiatry, Massachusetts General Hospital, Boston, MA, United States of America

* MK and MSW are Corresponding Authors

Email: marc.weinberg@mgh.harvard.edu (MSW); mkodali@mgh.harvard.edu (MK)

¶ MK and JA are Joint First Authors

& KJ, SD, and MSW are Joint Senior Authors

Abstract Cerebrospinal fluid (CSF) matrix biomarkers have become increasingly valuable surrogate markers of neuropsychiatric diseases in research and clinical practice. In contrast, CSF cells have been rarely investigated due to their relative scarcity and fragility, and lack of common collection and cryopreservation protocols, with limited exceptions for neurooncology and primary immune-based diseases like multiple sclerosis. the advent of a microfluidics-based multi-omics approaches to studying individual cells has allowed for the study of cellular phenotyping, intracellular dynamics, and intercellular relationships that provide multidimensionality unable to be obtained through acellular fluid-phase analyses. challenges to cell-based research include site-to-site differences in handling, storage, and thawing methods, which can lead to inaccuracy and inter-assay variability. In the present study, we performed single-cell RNA sequencing (10x Genomics) on fresh or previously cryopreserved human CSF samples from three alternative cryopreservation methods: Fetal Bovine Serum with Dimethyl sulfoxide (FBS/DMSO), FBS/DMSO after a DNase step (a step often included in epigenetic studies), and cryopreservation using commercially available Recovery© media. In comparing relative differences between fresh and cryopreserved samples, we found little effect of the cryopreservation method on being able to resolve donor-linked cell type proportions, markers of cellular stress, and overall gene expression at the single-cell level, whereas donor-specific differences were readily discernable. We further demonstrate the compatibility of fresh and cryopreserved CSF immune cell sequencing using biologically relevant sexually dimorphic gene expression differences by donor. Our findings support the utility and interchangeability of FBS/DMSO and Recovery cryopreservation with fresh sample analysis, providing a methodological grounding that will enable researchers to further expand our understanding of the CSF immune cell contributions to neurological and psychiatric disease.

INTRODUCTION

The lumbar puncture (LP) is a safe ambulatory procedure for collecting cerebrospinal fluid (CSF) [1]. LPs are classically applied to diagnosis of neurological diseases such as communicating hydrocephalus, autoimmune or infectious encephalitis, central nervous system vasculitis, and cancer [2]. Improvements in biomarker characterization [3] and their ultrasensitive detectability have increased the utility and promise of CSF for aiding in diagnosis for neuropsychiatric disorders [4], and for neurodegenerative diseases like Alzheimer's disease (Aβ42, t-Tau, and p-Tau181) [5], motor neuron disorders [6], and prion disease [7]. Given the recent United States Food and Drug Administration approval of several monoclonal antibody-based treatments against amyloid-β in Alzheimer's disease, and the requirement of either CSF- or amyloid-PET imaging-based biomarker thresholds for receiving lecanemab [8] and likely other similar forthcoming treatments, we anticipate that the clinical utilization of the lumbar puncture is likely to increase in the United States in coming years.

CSF is a clear fluid produced by the choroid plexus and ependymal cells lining the brain's ventricles. It is in continuous interchange with the brain's interstitial fluid as it circulates through subarachnoid and glymphatic spaces [9]. The acellular and cellular composition of CSF differs greatly from that of the peripheral blood, given multiple complex barriers between these compartments [10]. CSF cells are primarily of hematopoietic origin. In contrast to the peripheral blood, healthy CSF cellular composition is predominantly lymphoid cells such as CD4+ T cells, whereas myeloid lineage cells account for a lower proportion [11]. Few cells are found in CSF compared to blood, with estimates ranging between 1-3 cells/μL [12] in healthy individuals.

65 Single-cell-based transcriptomic and epigenetic methods provide high resolution and depth of
66 information about rare or underrepresented cell populations, unbiased assessment of cellular
67 heterogeneity, cell lineage and trajectory, and modeling of intercellular communications. With
68 the advent of single-cell RNA sequencing (scRNAseq), new CSF cell populations have been
69 identified [13,14], and possible mechanisms of neurodegenerative disease states have been
70 elucidated [15,16], with far greater sensitivity and depth of discovery than that enabled by related
71 cellular-based approaches such as flow cytometry [17]. Although using freshly acquired CSF
72 cells may be thought of as ideal, cryopreservation of CSF cells has many practical advantages,
73 such as the opportunity to provide inventory to biorepositories and share resources, reduction of
74 batch effects in cross-sectional analyses, and providing a means to perform longitudinal intra-
75 individual comparisons. However, there are concerns that the transcriptional makeup of the cells
76 will change during the cryopreservation or the thawing process. While there are reagents
77 available that could simplify and reduce batch effects in large studies through sample fixation at
78 the time of collection (e.g., 10x Genomics Fixed RNA Profiling [18]), such approaches rely on
79 probing against a limited subset of genetic targets [19] and may prohibit clonal analyses. To date,
80 several non-CSF-related studies have compared the quality of scRNAseq transcriptomic results
81 between cryopreserved and freshly captured cells using cells derived from peripheral
82 compartments including blood [20–25], generally showing the success of recapitulating fresh
83 cell-based analyses in cryopreserved samples. However, to our knowledge, only two studies have
84 compared fresh versus cryopreserved CSF cells [26,27]. The first study that demonstrated the
85 feasibility of using cryopreserved CSF scRNAseq did not directly compare fresh vs.
86 cryopreservation [26], whereas, the other study is limited to a technical evaluation with no
87 biological findings [27].

88 Cryopreservation agents include methanol, laboratory-prepared serum combined with dimethyl
89 sulfoxide (DMSO), or a purchasable storage medium (e.g., Recovery). Epigenetic analysis can
90 benefit from additional sample preparation, such as DNase incubation [28]. Here, we compared
91 transcriptomics results from multiple CSF donors seen in the outpatient setting to evaluate
92 possible normal pressure hydrocephalus (NPH). Their evaluation includes a large volume lumbar
93 puncture. Owing to the excess of fluid collected, we could divide CSF from each donor sample
94 into a fresh and one or more cryopreservation method samples, enabling a thorough comparison
95 of fresh to cryopreserved CSF cells. We report on cellular quality, cell-type proportions, and
96 differences in overall gene expression patterns by condition. we demonstrate the utility and
97 compatibility of various CSF cryopreservation techniques for identifying latent genetically based
98 differences in cellular transcription patterns.

99 Methods

100 Clinical methods

101 CSF samples were collected as excess fluid from lumbar punctures of patients receiving
102 care at the Mass General Hospital Memory Disorders Unit, as part of an NPH-related clinical
103 evaluation. All lumbar punctures were performed by SEA, using a 24-gauge Sprotte spinal
104 needle, with approximately 20-35mL CSF removed. The first several mL were used for clinical
105 labs and avoided for research purposes, given the risk of procedure-associated red blood cell
106 (RBC) contamination. Massachusetts General Brigham Institutional Review Board approved
107 research use, and informed consent was obtained from all donors.
108

109 CSF cell collection and storage

110 Fluid was collected in sterile 15 mL Falcon tubes and transferred on ice (approx. 30-45
111 min) prior to centrifugation. Samples were centrifuged at 300xg for 10 min at 4°C using a
112 swinging bucket rotor. All but 0.1 mL of fluid was removed, and the cell pellet was resuspended.
113 Cell viability and cell count were performed using Luna automated cell counter with acridine
114 orange and propidium iodide viability dye. Red blood cell contamination was determined by
115 subtracting the nucleated cells from the total cells. cell suspension was divided accordingly into
116 one of the below cryopreservation conditions alongside the fresh CSF cell fraction, with a
117 minimum of 5000 cells per condition. Fresh (FRE) CSF samples were immediately prepared for
118 running on the 10x controller. For cryopreservation conditions, the divided cellular fraction(s)
119 was cryopreserved at -80C in equal volumes of the following cryoprotectants: 1) FBS - cells
120 were stored in ice-cold Fetal Bovine Serum (FBS, Thermo-scientific, cat# A4766801) mixed
121 with 10% DMSO (cat# D2650), 2) REC – cells were stored in Recovery media (Thermo-
122 scientific, Cat# 12648010), 3) DNA – Cells were treated with 1X DNase (Stemcell, cat# 07900)
123 for 30 minutes at 22°C, then washed and spun at 3000xg for 6 minutes, followed by
124 cryopreservation in FBS mixed with 10% DMSO. Use of DNase is commonly recommended for
125 some epigenetic analyses [28]. Although we do not examine epigenetics here, we provide quality
126 control data regarding the use of DNase before FBS/DMSO cryopreservation. Methanol
127 cryopreservation based on previously established 10x protocols [29] led to poor thawed cell
128 recovery, leading us not to pursue this method further. Cryopreserved cells were warmed to near
129 complete thaw in a 37°C water bath, after which pre-warmed wash buffer (phosphate-buffered
130 saline supplemented with 1% bovine serum albumin and RNase inhibitor) was added (1.5 mL) to
131 the cryovial. Cells were resuspended and transferred to a 15mL falcon tube containing 9mL
132 warmed wash buffer. The cryovial was rinsed again with warmed wash buffer for further cell

133 recovery). Falcon tubes were centrifuged at 300xg at 4°C for 5 min. The supernatant was
134 removed, and cells were resuspended in 500 μL wash buffer and transferred to a smaller 1.5 ml
135 tube; 30 μL of the aliquot was removed and analyzed for viability and cell counts using Calcein-
136 AM and NucBlue Live ReadyProbes Reagent (Invitrogen, Carlsbad, CA). The sample was
137 centrifuged at 300xg at 4°C for 5 min, resuspended in wash buffer, and loaded into the 10x 5' v2
138 mix sans reverse transcriptase enzyme. Finally, reverse transcriptase was added, and the sample
139 was loaded onto the 10x chip K. See Fig 1a for CSF workflow. The list of subjects, as well as the
140 type of cryopreservation method(s) performed on each subject's CSF cells are listed in S1 Table.
141 The number of tested cryopreservation conditions was determined based on the total cell count.
142 Cryopreserved samples were prepared in parallel with the fresh running on the 10X controller
143 and run later after thawing and counting, within 12 months of initial cryopreservation.
144 Fresh or thawed cryopreserved CSF mixed with 10x 5' v2 RT Reagent Master Mix were
145 immediately processed with the 10x Genomics Chromium Next GEM Single Cell 5' v2 kit (10x
146 Genomics, Pleasanton, CA), cDNA amplified, and library constructed per the manufacturer's
147 protocol. Library quality control (QC) was based on Agilent Tapestation 4200 HS D1000
148 screentapes (Agilent Technologies, Waldbronn, Germany). Multiplexed library pool QC was
149 based on Agilent Tapestation 4200 HS D1000 and Kapa Library Quantification Kit for Illumina
150 platforms (Kapa BioSystems, Boston, MA) and sequenced at shallow depths on Illumina's iSeq
151 100 v2 flow cell for 26x10x10x90 cycles for estimated reads per cell. After demultiplexing,
152 libraries were rebalanced based on reads per cell. Normalized pool QC was based on Agilent
153 Tapestation 4200 HS D1000 and Kapa Library Quantification Kit for Illumina platforms and
154 high depth sequenced on Illumina's NovaSeq 6000 S4 v1.5 flow cell for 26x10x10x90 cycles, to
155 obtain a sequencing depth of 50K reads/cell (whole transcriptome libraries). Reads were aligned

156 to reference 2020-A (Ensembl 98) transcriptome and quantified using Cell Ranger v6.0.2 multi
157 pipeline. Further data processing and analysis were performed using the Seurat library (v 4.3.0)
158 [30–33]. ggplot2 [34] package was used to generate the visualizations in conjunction with Seurat
159 package. Quality control was performed on each sample: cells with less than 200 genes, more
160 than 4500 genes (presumed doublets), or greater than 20% mitochondrial transcripts were filtered
161 from further analysis. The average number of genes per cell was 1578. Red Blood Cell (RBC)
162 (defined as the cells that showed high expression of Hemoglobin genes HBA and HBB) were
163 manually removed from the analysis.
164
165 **Fig 1**. **scRNAseq of fresh and cryopreserved CSF cells.** a) Graphical schema depicting the
166 experimental design. Freshly collected CSF was spun and the resulting CSF cells were counted,
167 cells were then immediately divided into either FRE which was immediately processed on the
168 10x Chromium Controller to capture single cells or cryopreserved with protocols for FBS and/or
169 REC and/or DNA for downstream processing basing on the total cell count. The cryopreserved
170 fractions were later thawed and run on the 10x Chromium Controller, and the resulting data were
171 analyzed together. b) Uniform Manifold Approximation and Projection (UMAP) plot of all the
172 cells of samples from CSF A, B, and C, annotated to depict the FRE or FBS or REC protocols. c)
173 UMAP plot of all the cells of samples from CSF A, B, and C in protocols FRE, FBS and REC
174 annotated to depict the cell types clustered using Azimuth peripheral blood mononuclear cells
175 (PBMC) reference atlas at L1 resolution. d) Dot plot depicting the concordance between
176 respective cell-type specific enriched marker gene expression of all the cells from samples CSF
177 A, B, and C (on the y-axis) as characterized by earlier published CSF scRNAseq studies that are
178 correspondingly identified and clustered accordingly (on the x-axis) by Azimuth reference atlas
179 at L1 resolution.

Cell integration and data processing

Samples were integrated using the Seurat package v4.0 [35]. First *FindVariableFeatures()* was used to find the top 2000 highly variable genes. Then *SelectIntegrationFeatures()* was used to select features and PCA was performed using *RunPCA()* using the selected features. Reciprocal PCA was performed to identify pairwise anchors between the reference and the list of datasets using *FindIntegrationAnchors()*. Two fresh samples (CSF A and CSF C), one male and one female, both with high total counts of cells, were selected as anchors for data integration. Integration was performed using *IntegrateData(). NormalizeData()* was used for normalizing the count data for each dataset, with a scaling factor = 10000. Data was log-transformed before analysis. We used Azimuth [31], a reference atlas of human peripheral blood mononuclear cells (PBMCs), to define and annotate the CSF cell types. *RunAzimuth()* was used to map our data to PBMC reference dataset. This returned a Seurat object that contained cell annotations (at multiple levels of resolution), and prediction (i.e., confidence) scores for each annotation: This score was used for filtering cells with low confidence classifications. To validate the results of Azimuth-based cell type calling, we compared the Azimuth cell type annotations with commonly used immune cell marker genes, taken from recent CSF-based studies [15,16,36].

Normalized gene expression for these markers was further plotted using *Dotplot()* from the ggplot2 package. For obtaining overall gene expression correlation plots, average gene expression was calculated for each subject (CSF A, CSF B and CSF C) by each condition. Pearson method of correlation was used and the plots were visualized using *ggscatter()* in the ggplot2 package in R. Euclidean distance matrix was computed using *dist()* in stats (version

203 4.2.1). Hierarchical clustering was performed on the distance matrix by the complete clustering
204 method using *hclust()* in the stats package. We picked the genes HSPA1A, HSPA1B and
205 HSP90AA1, which are related to cell stress response pathways (GO:0031072 - heat shock
206 protein binding and GO:0051082 - unfolded protein binding) as published in an earlier study
207 [24], to compare the effect of cryopreservation. Global gene expression was plotted using Seurat
208 *VlnPlot()*. Differential gene expression analysis was performed between two conditions within a
209 cell cluster using Seurat *FindMarkers().* Significance was defined as Bonferroni-adjusted p-value
210 <0.05 and absolute log2 fold change >0.58 (fold change >1.5). We further picked the genes
211 XIST, KDM4D, UTY, DDX3Y and USP9Y, related to sex differences as published in the earlier
212 study [37], to find the similarities between differential expression analysis among all the
213 conditions together, as well as in each individual condition. *pheatmap()* was used to plot the
214 heatmap of differential expression.
215

216 Statistical analysis

217 Statistical tests were indicated where applicable for comparing quality control metrics.
218 One-way ANOVA and Tukey's multiple comparisons test were used for normally distributed
219 data, and Friedman's was used for the comparison of percentages. Statistical tests were
220 performed with GraphPad Prism v9.5.

221 RESULTS

222 Donor demographic and clinical characteristics

223 Donor ages ranged from 61-85 years (median age 74 years) at CSF collection. According
224 to self-report data recorded in electronic health records, all donors identified themselves as

225 white/Caucasian and 55% of donors were male. See S1 Table for individual donor demographic
226 and clinical information.

227 *CSF sample characteristics:* Average CSF volume was 28.7 mL (SD 8.04, range: 8-38 mL).
228 Total CSF cell counts averaged 1980/mL, (SD 1810, range: 570-6700/mL), RBC contamination
229 was overall low, averaging 754/mL, (SD 105, range: 0-305/mL). These data exclude two
230 samples, one for which RBC contamination in one sample was unusually high, enabling
231 visualization of a red pellet. This sample was removed from further analyses in this study. See S1
232 Fig for examples of cell pellets from spun CSF samples with and without RBC contamination.
233 The other sample with notably high RBC contamination was CSF F (43,500 RBCs/mL of CSF).
234 We included this sample for limited analysis (FBS vs REC comparison). CSF cell viability
235 averaged 99.29%, (SD 1.20, range 96.75-100%). Cells per condition averaged 10,600, (SD 2800,
236 range: 5000-16000 cells). Samples showing pleocytosis were divided into multiple
237 cryopreservation conditions. Sample details by donor and cryopreservation method can be found
238 in S1 Table. A total of 7 FRE, 11 FBS, 11 REC and 5 DNA, were obtained. Donors A, B, and C
239 each contributed at least one sample to the FRE, FBS, and REC conditions, allowing for a
240 within-subjects comparison of these conditions. Donors A, B, C, and J contributed samples for
241 FRE vs FBS comparison. Donors A, B, C, and H contributed samples for FRE vs REC
242 comparison. Donors A, B, C, D, E, F, and G contributed samples for FBS vs REC comparison.
243 Donors A, C, D, F, and G contributed samples for FBS vs DNA comparison.

244 Single-cell sample quality control metrics

245 Pre-filtering, total droplet-encapsulated cell count was 78,551, summing 16,279 FRE,
246 24,850 FBS, 27,756 REC, and 9666 DNA. Post-filtering by gene and mitochondrial transcript

247 count led to an overall cell count reduction of 1%. 21,117 genes were detected on average across
248 all samples, with 19,173 in FRE, 19,428 in FBS, 19,747 in REC, and 17,416 in DNA. The pre-
249 filtration average unique molecular identifiers (UMI) were 4,576 across all samples, with 6,230
250 in FRE, 4,062 in FBS, 3,788 in REC, and 5,248 in DNA. Filtration led to an increase in overall
251 average UMI by 1%. Pre-filtered average percent mito-based reads were 2.6% overall, with 1.9%
252 in FRE, 2.4% in FBS, 3.5% in REC, and 2.6% in DNAse. Filtration led to a decrease in average
253 percent mitochondrial reads of 1%. No significant differences were found between treatment
254 conditions, or in comparing pre- vs post-filtration metrics. We focus on comparisons between
255 CSF A, B, and C in our studies since these were the only donors for which the FRE, FBS, and
256 REC conditions were all available. CSF A, B, and C feature count (average genes per cell), UMI
257 count, and percent mitochondrial read distributions are graphed in S2a-c Figs. The average genes
258 detected per cell in 2041 in FRE, 1102 in FBS and 1273 in REC. There was an overall decrease
259 in the average genes detected per cell in both the cryopreservation conditions, but REC was
260 found to be significant (one way ANOVA, Tukey's Posthoc test, $p = 0.0031$). UMI was overall
261 higher in FRE than FBS and REC groups, though this was not significant statistically: $F(1.20,$
262 $2.401) = 8.86$, $p=0.08$. There were no differences in the percentage of mitochondrial reads across
263 the three groups ($p=0.94$). Features, UMI, and percent mitochondrial reads were very similar
264 between FBS and REC (including samples CSF A-G, see S4b Fig), and between FBS and DNA
265 conditions (including samples CSF A, C, D, and G, see S5b Fig). See S2 Table for detailed
266 quality control-based metrics for each donor, condition, and sample replicate. Examination of
267 global heat shock protein genes HSPA1A, HSPA1B, and HSP90AA1 found minimal to no
268 differences in gene expression by cryopreservation method in any of the three donors (S2d Fig).

Fig 2. Distribution and cellular type proportions of cryopreserved versus freshly captured CSF cells. a) UMAP plot of all the cells in samples CSF A, B, and C from FRE, FBS, and REC protocols were annotated to show the cell types clustered using Azimuth PBMC reference atlas [35] at the L1 resolution. b) Stacked bar plots depicting the individual cell type proportions obtained after clustering using Azimuth reference atlas at the L1 resolution in samples CSF A, B and C from FRE, FBS and REC protocols.

CSF cell types

Integrated CSF cells from donors A, B, and C, colored by fresh or cryopreservation conditions, are visualized by UMAP plot in Fig 1B. The cell types defined by Azimuth L1 supervised clustering are shown in Fig 1C. The samples represent all L1 cell types, including CD4 and CD8 T cells, monocytes, dendritic cells, NK cells, and scant B-cells. Few cells fell into 'other' or 'other-T' categories by the L1 algorithm. We provide several methods of validation of the Azimuth-based method. First, we cross-validated Azimuth-based cell designations to cell type markers from the literature (see METHODS). The Azimuth L1-based cell type predictions are concordant with established phenotypic markers. Next, we prepared an adjacency table by donor, condition, sample, and Azimuth-derived cell type. L1- and L2-resolution cell designations are provided (L2 information is provided as an additional resource but is not utilized for further data analysis in this study). Mean predicted scores, a confidence metric in cell type callings by Azimuth, ranged from 78-88%. By cell type (%) in descending order of percent presence in sample: CD4 T (87), Mono (83), CD8 T (87), DC (11), B (78), Other (57), Other T (67), and NK (78). The cryopreservation method (including FBS, REC, DNA) did not affect mean predicted scores (S3 Table).

291 ## Effects of cryopreservation method on cellular proportions

292 UMAP and stacked bar-plots of the Azimuth L1-based cell type by cryopreservation
293 method and donor are shown in Fig 2A and Fig 2B respectively. Overall, all cell types were
294 identified across all donors and conditions. There were generally even distributions of cell
295 proportions by cryopreservation method across donors. Based on the comparison of cell type
296 proportions (Fig 2b) FBS cryopreserved samples appeared to have slightly greater proportions of
297 monocytes and lower proportions of CD4 T cells than FRE or REC samples across donors.
298 However, this was not found to be significant by statistical test (monocytes: p=0.19, and CD4 T
299 cells: p=0.19). Examining the raw cell counts (S2 Table), these proportional differences seem to
300 be related to a selective loss of lymphocytic cells. For instance, in two independently prepared
301 samples of CSF A FRE, there were 1266 and 1240 monocytes, with 1233 and 1308 CD4 cells,
302 respectively. The FBS samples had fewer overall cells, with 1059 and 1888 monocytes, but
303 fewer CD4 cells: 958 and 833, as compared to monocytes. DNAse-treated samples,
304 cryopreserved similarly to FBS samples, showed fewer CD4 cells: 866 and 1190 than
305 monocytes: 1164 and 1471. REC cryopreservation looked more like FRE: 1119 and 780
306 monocytes, with 1089 and 1151 CD4 cells. Comparing FBS to REC (S4c Fig), the phenomenon
307 of slightly lower CD4 T cell proportions in FBS than REC is maintained. There is no consistent
308 difference between cell proportions in comparing DNase pre-treated samples to FBS (S5c Fig).

309 In contrast to the limited differences in cell proportions by cryopreservation method,
310 donor-specific biological differences are preserved, and marked. For instance, CSF C shows far
311 greater proportion of CD4 T cells, and proportionately fewer monocytes than CSF A and B. A
312 dotplot stratifying CSF samples by cryopreservation method and Azimuth L1 cell type is
313 presented in S3 Fig. Dots showing average gene expression reveal highly similar cell type

314 marker expression and percent expression across cryopreservation methods compared to the
315 fresh condition.
316

317 Effects of cryopreservation method on global gene expression

318 To answer whether the cryopreservation method affected global gene expression, we
319 prepared a hierarchical clustering dendrogram comparing global (across all cell types) gene
320 expression across FRE, FBS, and REC conditions for CSF A, B, and C (Fig 3a). Samples
321 obtained from the same donor using different cryopreservation methods clustered together,
322 indicating that the observed variations in global gene expression profiles are primarily due to
323 biological variability rather than technical factors (similarity matrix is provided in S4 Table,
324 lower scores indicate closer cluster distance). We next correlated global gene expression within
325 donors between FRE and cryopreserved conditions (Fig 3b), finding very high correlations
326 between FRE and FBS, and FRE and REC conditions (average R-value: 0.98, Range: 0.94 – 1).
327

328 **Fig 3. Comparison of overall gene expression between cryopreserved and fresh CSF**
329 **samples.** a). Dendrogram showing the hierarchical clustering of relative sample to sample
330 distances in samples CSF A, B, and C in FRE, FBS, and REC protocols. Note the companion
331 adjacency matrix found in S4 Table. b). Scatter plots with correlation statistics of FRE vs FBS
332 and FRE vs REC global gene expression in samples CSF A, B and C.

333 Effect of cryopreservation on revealing latent sex-linked expression

334 To test whether the cryopreservation method impacted our ability to extrapolate
335 functional or biologically meaningful data, we utilized established knowledge regarding sexually
336 dimorphic gene expression: XIST found on the X-chromosome and KDM4D, UTY, DDX3Y,

337 and USP9Y on the Y chromosome. We analyzed CSF A, B, and C samples (FRE, FBS, and REC
338 conditions) to identify differentially expressed genes between males and females (Fig 4A). We
339 evaluated CD4 cells as exemplars given their abundance in CSF. We observe many sexually
340 dimorphic genes (n = 149 upregulated and 124 downregulated genes based on male/female fold
341 change). Each sex-specific gene of interest was in the expected direction (genes shown in red on
342 the right side of the volcano plot indicate higher expression in males). These results demonstrate
343 that combining samples prepared using different cryopreservation strategies did not affect the
344 detection of sexually dimorphic gene expression. We next determined whether cryopreservation-
345 specific conditions are independently capable of detecting sexually dimorphic gene expression
346 differences. To do this, we collapsed all cell types together and compared cryopreservation
347 conditions. As seen in Fig 4b, the fold change differences between sexes for the five sex-linked
348 genes of interest showed highly similar patterns across the various cryopreservation methods.
349 They compared favorably to combinatory and FRE results.

350 **Fig 4. Differential gene expression analysis of sexually dimorphic genes from fresh and**
351 **cryopreserved CSF samples.** a) Volcano plot showing the significant (p-adjusted < 0.05,
352 Log2FC > 0.58) differentially expressed genes between males and females in CSF A, B, and C
353 CD4+ T-cells combining all fresh and frozen samples. Genes upregulated in males are colored
354 red, and downregulated in males are colored blue. Grey dots indicate the non-significant genes.
355 b) Heatmap showing the average log2fold changes of the sexually dimorphic genes XIST,
356 KDM4D, UTY, DDX3Y, and USP9Y from differential gene expression analysis of CD4+ T-
357 cells in CSF A, B and C for All samples (FRE, FBS and REC combined), and stratified by FRE,
358 FBS, and REC.

359 # Discussion

360 In this methodological study of CSF cells donated by patients receiving evaluations for
361 possible normal pressure hydrocephalus, we compared various cryopreservation approaches to
362 freshly run CSF cells through the scRNAseq process. We used three cryopreservation methods,
363 including two cryopreservation agents (FBS/DMSO and Recovery media). We included an
364 additional DNase step prior to FBS/DMSO cryopreservation given this step's known benefit on
365 the quality of epigenetic analyses. Overall, we found little impact of cryopreservation on cell
366 integrity and stress, cell type representation, or overall gene expression. Nuanced findings of the
367 study include possible relative losses of CD4+ T-cells using the FBS/DMSO cryopreservation
368 technique, and limited loss of sequencing depth, as seen by relatively lower average UMI in all
369 cryopreserved samples. The robustness and interchangeability of cryopreserved and freshly run
370 samples was demonstrated using an example of sexually dimorphic gene expression, which was
371 noted using a combined dataset from fresh and pre-frozen samples, as well as by stratified
372 analysis by cryopreservation method. When compared to the fresh condition, there were no
373 apparent differences due to cryopreservation methods using FBS/DMSO, Recovery media, or
374 from prior DNase treatment. Our data support the ability to cryopreserve and later utilize CSF
375 cell samples, enabling batched single-cell analyses for wide-ranging cellular and molecular-
376 based advances in neurological, oncological, infectious disease, and psychiatric research.

377 Effect of cryopreservation on cellular stress, and sequencing quality

378 In the present study, we noted limited to no impacts of cryopreservation on evidence of
379 cell stress, and our data supported overall robust single cell transcriptome results. For
380 comparison, in the preprinted study by Touil et al., [27], researchers recovered approximately
381 70% of cryopreserved cells, without other notable impacts of cryopreservation on mitochondrial
382 reads. We similarly routinely find approximately 70% cell recovery (not shown) post-thaw, and

383 likewise do not find any evidence of increased cellular stress, as represented by the proportion of
384 mitochondrial reads. We also find that global expression of cellular stress response proteins,
385 including heat-shock proteins HSPA1A, HSPA1B, and HSP90AA1 was unaffected by FBS or
386 REC cryopreservation. Previous studies have noted upregulation of cellular stress pathways in
387 cryopreserved dissociated tumors [24] or single-cell subpopulations of peripheral blood
388 mononuclear cells. PBMCs [22]. The latter study noted that while the effects appeared limited
389 and did not disrupt key aspects of the cellular subpopulation, cell populations showing evidence
390 of cellular stress clustered uniquely from healthy cells, allowing for selective filtration.
391 Differences in thawing and cryopreservation strategies used across ours and previous studies are
392 likely to account for differences in cellular stress pathway activation; this supports the
393 importance of consistency in sample treatment surrounding cryopreservation practice (e.g.,
394 temperature control, spin speed, and freezing and thawing schedule).

395 Non-viable cells are readily identified using hemocytometers and dye markers. Generally, we
396 find >90% cell viability in CSF cells. The differences between recovery and viability are likely
397 related to the degradation of damaged cells during post-thaw washes. The report by Touil et al.,
398 [27] also notes higher hemoglobin gene expression in fresh samples despite excluding RBCs
399 from analyses. Our dataset reveals a similar phenomenon (not shown). We further note from
400 other optimization studies in our labs that increasing the temperature of centrifugation (i.e., room
401 temperature) decreases overall cell viability substantially (20-30% pre-freeze), with the greatest
402 effect on RBC viability (data not shown). This selective effect can mask peripheral blood
403 contamination, leading to a false interpretation of peripheral contamination as CSF-specific cells.
404 Use of an atraumatic LP technique and avoiding using the first several mL of collected CSF can
405 prevent peripheral blood contamination, and maintenance of 4C of the sample through

406 cryopreservation is essential. Unbiased identification and filtration of cells containing
407 unexpected or ambient gene expression, such as hemoglobin, may be practically useful, but
408 should also be applied with caution given the underlying possibility of such findings reflecting
409 peripheral blood contamination. Finally, both groups identified a limited but consistent decrease
410 in UMIs and genes from cryopreservation. We find this to be consistent between FBS/DMSO
411 and Recovery media as compared to Fresh samples. We attribute this to slight RNA degradation
412 occurring in the lengthier processing and sample preparation time required during thawed
413 samples.

414 Effects of cryopreservation on cellular proportion

415 We find very limited effects of cryopreservation on cell proportions. A careful evaluation
416 revealed non-statistically significant relative losses of CD4+ T cells in FBS/DMSO
417 cryopreserved samples versus fresh samples, with sparing of this phenomenon using Recovery
418 media. Oh et al., [26] compared Recovery to fresh, and did not evaluate FBS/DMSO. Like our
419 findings, they did not note any impact of Recovery media on CD4+ T cells. Rather, they noted an
420 overall low proportion of myeloid cells (6%) and noted mild losses of myeloid cells post-thaw
421 from Recovery cryopreservation. Our study finds greater proportions of CSF myeloid cells
422 (including an average of 27% monocytes). Several donors had far lower monocyte proportions
423 present in their CSF (e.g., CSF F [3%], and CSF C [6%]). Our findings are unlikely due to
424 miscalling of cell type, given both the substantial variability of monocyte proportions found in
425 our donor population, as well as the high mean predicted score (0.87) of Azimuth nearest-
426 neighbor calling, and our added validation of the Azimuth [31] functions using cell marker genes
427 used for cluster labeling in many scRNAseq studies.

428 # Limitations

429 This study has several limitations. First, we recognize that to perform comparative
430 analyses of freshly run versus cryopreserved CSF samples, many cells per donor are required.
431 This may bias our samples towards individuals showing CSF pleocytosis, limiting the
432 applicability of our results to healthy individuals. Next, although we carefully validate our cell
433 populations, a higher standard of cell marker-based identification would rely on a
434 transcriptionally-independent means of cell identification, such as through simultaneous epitope
435 and transcriptome measurement in single cells (i.e., CITE-seq) [27]. Lastly, while we find little
436 impact of cryopreservation on basal CSF cell transcriptomics, we cannot account for differences
437 in cellular function that would readily be revealed by functional cellular assays [32].

438 # Conclusion

439 In this methodological study of scRNAseq of CSF cells, we find good comparability
440 between cryopreserved and fresh preparations. Sufficient starting volumes of samples, delicate
441 cell isolation, rigid adherence to cryopreservation and thawing steps, and routine quality control
442 steps allow for the robust study of CSF cells, allowing for reduced assay-based variability, and
443 perhaps allowing for great leaps in diagnostic and mechanistic advances in many research
444 domains relating to the central nervous system's immune milieu.

445 # Acknowledgements

446 Sponsors were not involved in the design and conduct of the study, collection, management,
447 analysis, and interpretation of the data; preparation, review, or approval of the manuscript; or
448 decision to submit the manuscript for publication.

References

1. Engelborghs S, Niemantsverdriet E, Struyfs H, Blennow K, Brouns R, Comabella M, et al. Consensus guidelines for lumbar puncture in patients with neurological diseases. Alzheimer's Dement Diagnosis, Assess Dis Monit. 2017;8: 111–126. doi:10.1016/J.DADM.2017.04.007

2. Deisenhammer F, Bartos A, Egg R, Gilhus NE, Giovannoni G, Rauer S, et al. Guidelines on routine cerebrospinal fluid analysis. Report from an EFNS task force. Eur J Neurol. 2006;13: 913–922. doi:10.1111/j.1468-1331.2006.01493.x

3. Costerus JM, Brouwer MC, van de Beek D. Technological advances and changing indications for lumbar puncture in neurological disorders. Lancet Neurol. 2018;17: 268–278. doi:10.1016/S1474-4422(18)30033-4

4. Rømer TB, Jeppesen R, Haubo R, Christensen B, Benros ME. Biomarkers in the cerebrospinal fluid of patients with psychotic disorders compared to healthy controls: a systematic review and meta-analysis. Mol Psychiatry 2023. 2023; 1–14. doi:10.1038/S41380-023-02059-2

5. Olsson B, Lautner R, Andreasson U, Öhrfelt A, Portelius E, Bjerke M, et al. CSF and blood biomarkers for the diagnosis of Alzheimer's disease: a systematic review and meta-analysis. Lancet Neurol. 2016;15: 673–684. doi:10.1016/S1474-4422(16)00070-3

6. Agah E, Saleh F, Sanjari Moghaddam H, Saghazadeh A, Tafakhori A, Rezaei N. CSF and blood biomarkers in amyotrophic lateral sclerosis: protocol for a systematic review and meta-analysis. Syst Rev. 2018;7. doi:10.1186/S13643-018-0913-4

7. Satoh K. CSF biomarkers for prion diseases. Neurochem Int. 2022;155: 105306. doi:10.1016/J.NEUINT.2022.105306

8. Cummings J, Apostolova L, Rabinovici GD, Atri A, Aisen P, Greenberg S, et al. Lecanemab: Appropriate Use Recommendations. J Prev Alzheimer's Dis. 2023. doi:10.14283/JPAD.2023.30

9. Wright EM. Transport processes in the formation of the cerebrospinal fluid. Rev Physiol Biochem Pharmacol. 1978;83: 3–34. doi:10.1007/3-540-08907-1_1

473 10. Solár P, Zamani A, Kubíčková L, Dubový P, Joukal M. Choroid plexus and the blood-cerebrospinal fluid
474 barrier in disease. Fluids Barriers CNS. 2020;17. doi:10.1186/S12987-020-00196-2

475 11. Ransohoff RM, Engelhardt B. The anatomical and cellular basis of immune surveillance in the central
476 nervous system. Nat Rev Immunol. 2012;12: 623–635. doi:10.1038/nri3265

477 12. Wick M, Gross CC, Isenmann S, Strik H. Liquorzytologie: Standards, Stellenwert und moderne Methoden
478 [Cytology of cerebrospinal fluid : Standards, importance and modern methods]. Nervenarzt. 2016;87: 1276–
479 1281. Available: http://link.springer.com/10.1007/s00115-016-0219-5

480 13. Esaulova E, Cantoni C, Shchukina I, Zaitsev K, Bucelli RC, Wu GF, et al. Single-cell RNA-seq analysis of
481 human CSF microglia and myeloid cells in neuroinflammation. Neurol Neuroimmunol neuroinflammation.
482 2020;7. doi:10.1212/NXI.0000000000000732

483 14. Farhadian SF, Mehta SS, Zografou C, Robertson K, Price RW, Pappalardo J, et al. Single-cell RNA
484 sequencing reveals microglia-like cells in cerebrospinal fluid during virologically suppressed HIV. JCI
485 insight. 2018;3. doi:10.1172/jci.insight.121718

486 15. Gate D, Saligrama N, Leventhal O, Yang AC, Unger MS, Middeldorp J, et al. Clonally expanded CD8 T
487 cells patrol the cerebrospinal fluid in Alzheimer's disease. Nature. 2020/01/10. 2020;577: 399–404.
488 doi:10.1038/s41586-019-1895-7

489 16. Piehl N, van Olst L, Ramakrishnan A, Teregulova V, Simonton B, Zhang Z, et al. Cerebrospinal fluid
490 immune dysregulation during healthy brain aging and cognitive impairment. Cell. 2022;185: 5028-5039.e13.
491 doi:10.1016/J.CELL.2022.11.019

492 17. De Graaf MT, De Jongste AHC, Kraan J, Boonstra JG, Smitt PAES, Gratama JW. Flow cytometric
493 characterization of cerebrospinal fluid cells. Cytom Part B Clin Cytom. 2011;80B: 271–281.
494 doi:10.1002/CYTO.B.20603

495 18. 10x Genomics. Single cell gene expression on more samples with no time constraints. [cited 20 Jul 2023].
496 Available: https://pages.10xgenomics.com/rs/446-PBO-704/images/10x_Product-Sheet_LIT000159_Fixed-
497 RNA-Profiling_Letter_Digital.pdf

498 19. Wallace A. Single Cell Gene Expression Flex: Lock in cell states, unlock potential. 2022 [cited 20 Jul 2023].
499 Available: https://www.10xgenomics.com/blog/single-cell-fixed-rna-profiling-lock-in-cell-states-unlock-
500 potentialllace

501 20. Guillaumet-Adkins A, Rodríguez-Esteban G, Mereu E, Mendez-Lago M, Jaitin DA, Villanueva A, et al.
502 Single-cell transcriptome conservation in cryopreserved cells and tissues. Genome Biol. 2017;18.
503 doi:10.1186/S13059-017-1171-9

504 21. Wohnhaas CT, Leparc GG, Fernandez-Albert F, Kind D, Gantner F, Viollet C, et al. DMSO
505 cryopreservation is the method of choice to preserve cells for droplet-based single-cell RNA sequencing. Sci
506 Rep. 2019;9. doi:10.1038/s41598-019-46932-z

507 22. Lee JS, Yi K, Ju YS, Shin EC. Effects of cryopreservation and thawing on single-cell transcriptomes of
508 human T cells. Immune Netw. 2020;20: 1–8. doi:10.4110/in.2020.20.e34

509 23. Morsey B, Niu M, Dyavar SR, Fletcher C V., Lamberty BG, Emanuel K, et al. Cryopreservation of
510 microglia enables single-cell RNA sequencing with minimal effects on disease-related gene expression
511 patterns. iScience. 2021;24. doi:10.1016/j.isci.2021.102357

512 24. Wu SZ, Roden DL, Al-Eryani G, Bartonicek N, Harvey K, Cazet AS, et al. Cryopreservation of human
513 cancers conserves tumour heterogeneity for single-cell multi-omics analysis. Genome Med. 2021;13.
514 doi:10.1186/S13073-021-00885-Z

515 25. Chen D, Abu Zaid MI, Reiter JL, Czader M, Wang L, McGuire P, et al. Cryopreservation Preserves Cell-
516 Type Composition and Gene Expression Profiles in Bone Marrow Aspirates From Multiple Myeloma
517 Patients. Front Genet. 2021;12. doi:10.3389/FGENE.2021.663487/FULL

518 26. Oh H, Leventhal O, Channappa D, Henderson VW, Wyss-Coray T, Lehallier B, et al. Methods to investigate
519 intrathecal adaptive immunity in neurodegeneration. Mol Neurodegener. 2021;16. doi:10.1186/S13024-021-
520 00423-W

521 27. Touil H, Roostaei T, Calini D, Diaconu C, Epstein S, Raposo C, et al. A structured evaluation of
522 cryopreservation in generating single-cell transcriptomes from cerebrospinal fluid. Cell Reports Methods.

523 2023;3: 100533. doi:10.1016/J.CRMETH.2023.100533

524 28. Grandi FC, Modi H, Kampman L, Corces MR. Chromatin accessibility profiling by ATAC-seq. Nat Protoc.
525 2022;17: 1518–1552. doi:10.1038/s41596-022-00692-9

526 29. 10xGenomics.com. Methanol Fixation of Cells for Single Cell RNA Sequencing. [cited 5 Oct 2023] pp.
527 CG000136-Rev D. Available:
528 https://assets.ctfassets.net/an68im79xiti/6cAxyOjiQYyACGy89S5GbT/eabec33793e54441b0067f81df4eae9
529 3/CG000136_Demonstrated_Protocol_MethanolFixationCells_RevD.pdf

530 30. Hao Y, Hao S, Andersen-Nissen E, Mauck III WM, Zheng S, Butler A, et al. Integrated analysis of
531 multimodal single-cell data. Cell. 2021;184: 3573-3587. e29.

532 31. Stuart T, Butler A, Hoffman P, Hafemeister C, Papalexi E, Mauck WM, et al. Comprehensive Integration of
533 Single-Cell Data. Cell. 2019;177: 1888-1902.e21. doi:10.1016/j.cell.2019.05.031

534 32. Butler A, Hoffman P, Smibert P, Papalexi E, Satija R. Integrating single-cell transcriptomic data across
535 different conditions, technologies, and species. Nat Biotechnol. 2018;36: 411–420. doi:10.1038/nbt.4096

536 33. Satija R, Farrell JA, Gennert D, Schier AF, Regev A. Spatial reconstruction of single-cell gene expression
537 data. Nat Biotechnol. 2015;33: 495–502. doi:10.1038/nbt.3192

538 34. Wickham H. ggplot2: Elegant Graphics for Data Analysis. Applied Spatial Data Analysis with R. New
539 York: Springer-Verlag; 2008. Available: https://ggplot2.tidyverse.org

540 35. Hao Y, Hao S, Andersen-Nissen E, Mauck WM, Zheng S, Butler A, et al. Integrated analysis of multimodal
541 single-cell data. Cell. 2021;184: 3573-3587.e29. doi:10.1016/j.cell.2021.04.048

542 36. Heming M, Li X, Räuber S, Mausberg AK, Börsch AL, Hartlehnert M, et al. Neurological Manifestations of
543 COVID-19 Feature T Cell Exhaustion and Dedifferentiated Monocytes in Cerebrospinal Fluid. Immunity.
544 2021;54: 164-175.e6. doi:10.1016/j.immuni.2020.12.011

545 37. Vawter MP, Evans S, Choudary P, Tomita H, Meador-Woodruff J, Molnar M, et al. Gender-Specific Gene
546 Expression in Post-Mortem Human Brain: Localization to Sex Chromosomes. Neuropsychopharmacology.
547 2004;29: 373–384. doi:10.1038/sj.npp.1300337

548

549 # Supporting information

550 **S1 Fig. Representative images of the CSF cell pellet visible post-centrifugation.** See TIFF
551 file. A sample devoid of RBC contamination is seen on the left, and one with substantial RBC
552 contamination is seen on the right.

553 **S1 Table. Donor demographics and sample information.** See xlxs file. Subject IDs, Age, Sex,
554 and number of individual reactions tested from FRE, FBS, REC, and DNA samples listed.

555 **S2 Table. Quality control metrics pre- and post-filtration.** See xlsx file. QC filtering: Cells
556 having 200 – 4500 umi counts, < 20% mito genes detected were retained. 2000 high variable
557 genes were used for clustering. Columns: Total_cells.before.filtering: cells pre-filtering; cells
558 after filtering: cells remaining after application of above filters; Total_genes: Genes per sample,
559 avg_numi: average number of umi counts before filtering; numi after filtering: average number
560 of umi counts after filtering; avg_mito: average mitochondrial genes in each sample before
561 filtering; mito after filtering: average number of mitochondrial genes in each sample after
562 filtering.

563 **S2 Fig. Cellular features, UMI, mitochondrial reads, and cellular stress-related gene**
564 **expression.** See TIFF file. All graphs include data from CSF A, B, and C. (a-c) Density plot
565 showing the distribution of the number of transcriptional features (genes), number of Unique
566 Molecular Identifiers (UMI), and percentage of overall gene expression attributed to
567 mitochondrial genes, respectively. (d-f) Violin plots of normalized gene expression levels of
568 HSPA1A, HSPA1B, and HSP90AA1, respectively.

569 **S3 Table. Cell type designations, proportions and mean predicted scores.** See xlsx file. Mean
570 predicted score is the Azimuth-derived confidence score for a given annotation. 'All' refers to
571 the total of all cell types (L1 or L2). Columns E-L reference L1 designations (used throughout
572 the manuscript), and columns M-AP list L2 designations (not used elsewhere in the manuscript).
573 Summary information for samples by fresh or cryopreservation method can be found in the
574 lowest rows.

575 **S3 Fig. Concordance of cell type markers between cryopreserved and freshly run samples**.
576 See TIFF file. Dot plot comparison of cell-type specific enrichment of marker gene expression in
577 FRE, FBS, and REC protocols for samples CSF A, B, and C. Cell-type specific marker gene
578 expression and associated cell types are listed on the y-axis, and Azimuth reference atlas cell
579 designations at L1 resolution are listed on the x-axis.

580 **S4 Table. Dendrogram adjacency matrix of overall sample gene expression.** See xlsx file.
581 The order of the donors and fresh/cryopreservation condition is based on the unweighted
582 Euclidian distance between samples as visualized on the dendrogram (Fig 3a).

583 **S4 Fig. FBS versus Recovery comparisons.** See TIFF file. **(**a) UMAP plot of all the cells in
584 samples CSF A, B, C, D, E, F, and G from FBS and REC protocols were annotated to show the
585 cell types that were clustered using Azimuth PBMC reference atlas at L1 resolution. (b) Density
586 plot showing the similar distribution of the number of genes, number of unique transcripts, and
587 percentage of mitochondrial genes in all the cells from FBS and REC protocols in samples CSF
588 A, B C, D, E, F, and G. (c) Stacked bar plot depicting the individual cell type proportions
589 obtained after clustering using Azimuth reference atlas at L1 resolution in samples CSF A, B C,
590 D, E, F and G from FBS and REC protocols.

591 **S5 Fig. FBS versus FBS with Dnase (DNA) comparisons.** See TIFF file. (a) UMAP plot of all
592 the cells in samples CSF A, C, D, and G from FBS and DNA protocols were annotated to show
593 the cell types clustered using Azimuth PBMC reference atlas at L1 resolution. (b) Density plot
594 showing the similar distribution of the number of genes, number of unique transcripts, and
595 percentage of mitochondrial genes in all the cells from FBS and DNA protocols in samples CSF
596 A, B C, D, E, F, and G. (c) Stacked bar plot depicting the individual cell type proportions
597 obtained after clustering using Azimuth reference atlas at L1 resolution in samples CSF A, C, D,
598 and G from FBS and DNA protocols.

599

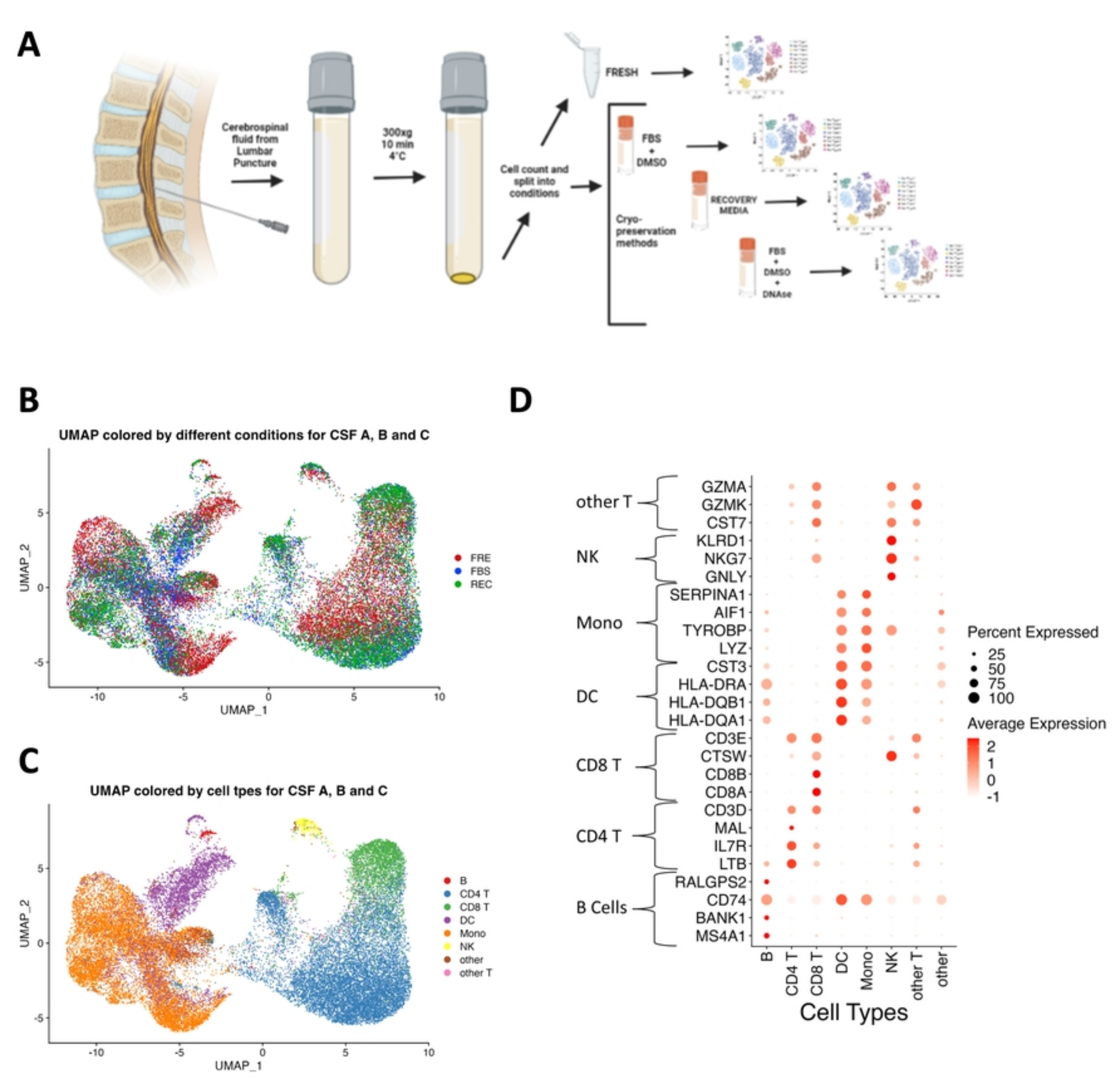
A
Cerebrospinal fluid from Lumbar Puncture
300xg 10 min 4°C
Cell count and split into conditions
FRESH
FBS + DMSO
RECOVERY MEDIA
FBS + DMSO + DNAse
Cryo-preservation methods
B
UMAP colored by different conditions for CSF A, B and C
FRE
FBS
REC
UMAP_1
UMAP_2
C
UMAP colored by cell tpes for CSF A, B and C
B
CD4 T
CD8 T
DC
Mono
NK
other
other T
D
other T
NK
Mono
DC
CD8 T
CD4 T
B Cells
GZMA
GZMK
CST7
KLRD1
NKG7
GNLY
SERPINA1
AIF1
TYROBP
LYZ
CST3
HLA-DRA
HLA-DQB1
HLA-DQA1
CD3E
CTSW
CD8B
CD8A
CD3D
MAL
IL7R
LTB
RALGPS2
CD74
BANK1
MS4A1
Percent Expressed
25
50
75
100
Average Expression
2
1
0
-1
Cell Types

Figure 1

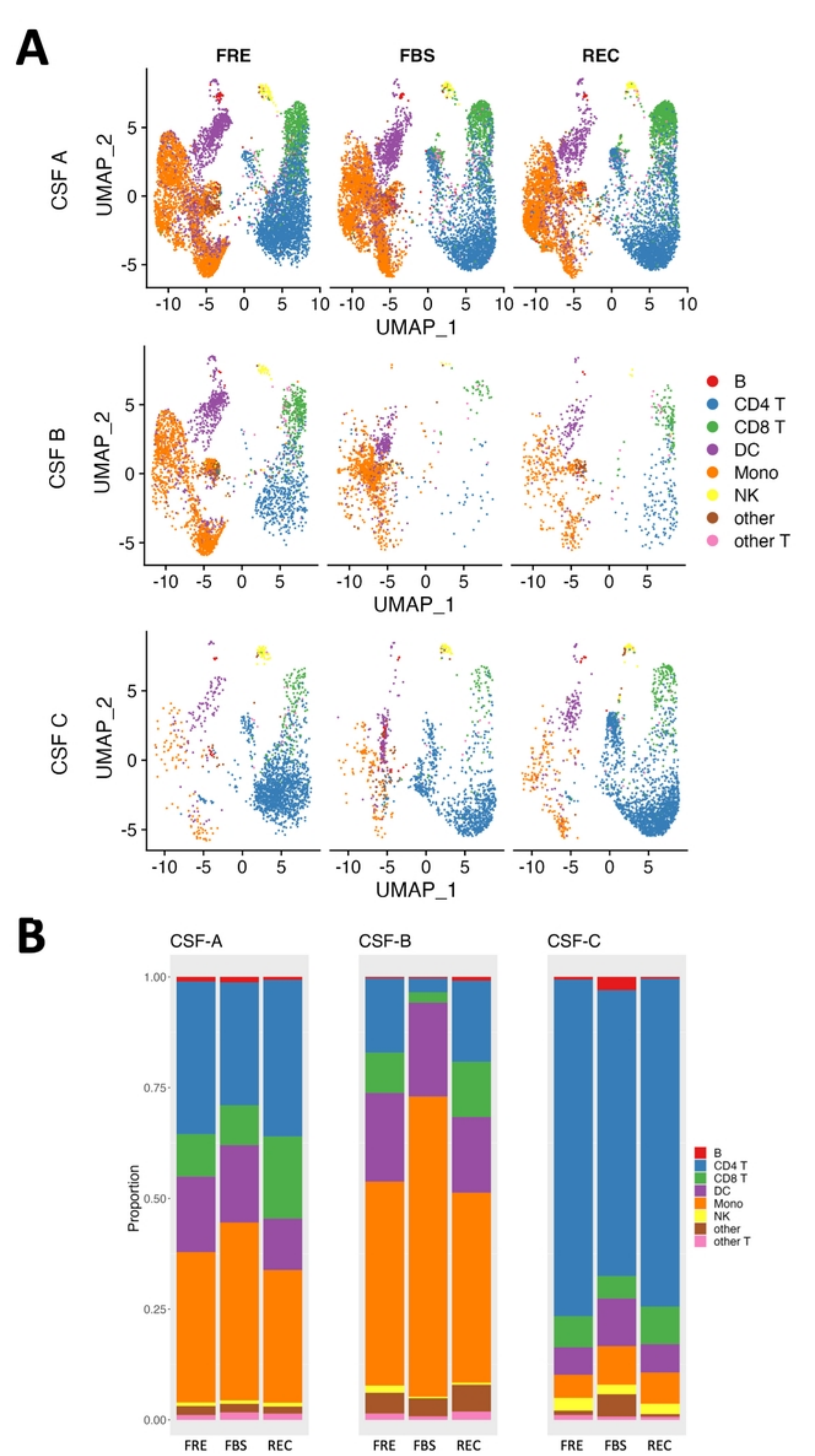
A
FRE
FBS
REC
CSF A
CSF B
CSF C
UMAP_2
UMAP_1
B
CD4 T
CD8 T
DC
Mono
NK
other
other T
B
CSF-A
CSF-B
CSF-C
Proportion
1.00
0.75
0.50
0.25
0.00
FRE
FBS
REC

Figure 2

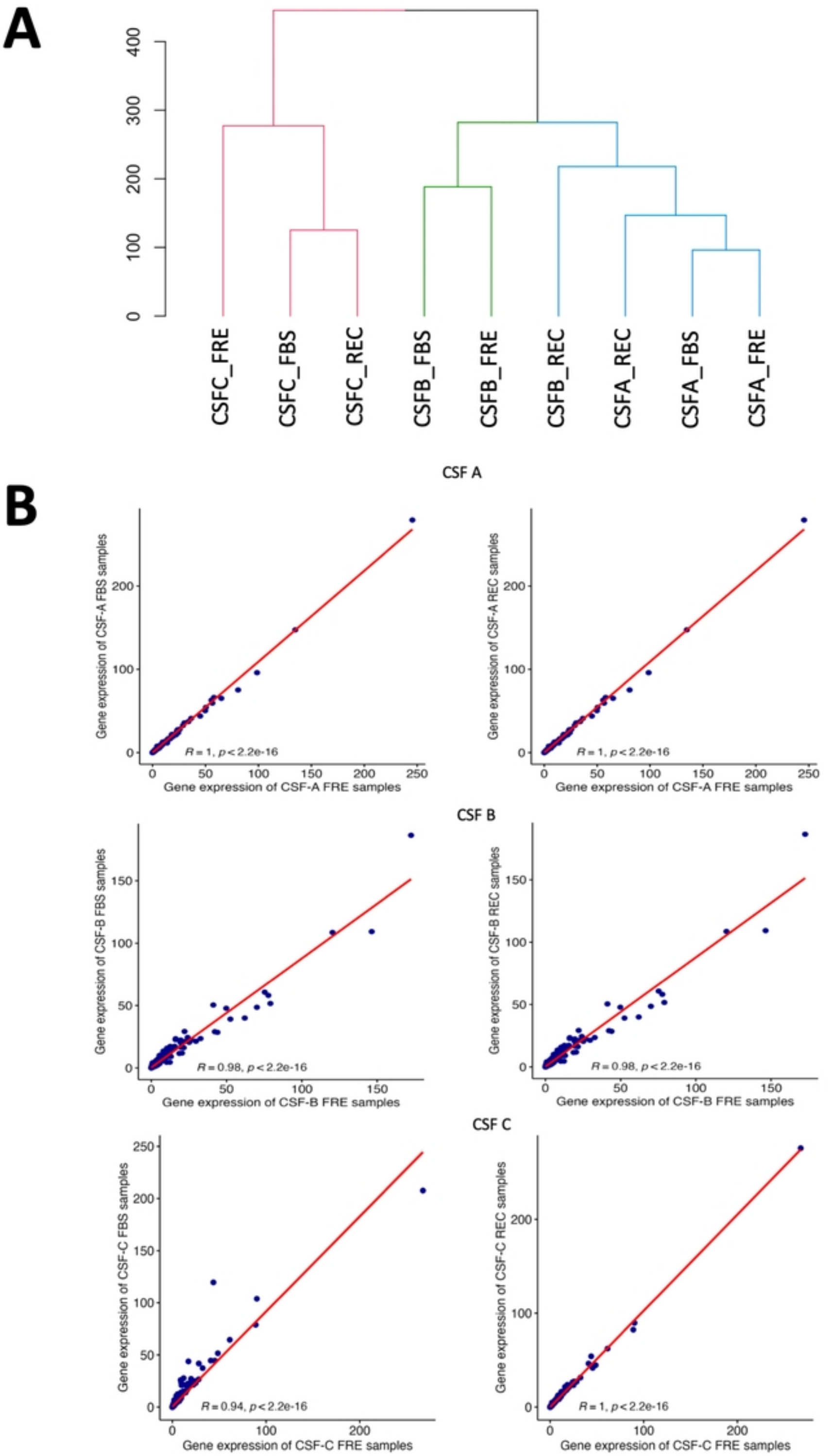
A
0
100
200
300
400
CSFC_FRE
CSFC_FBS
CSFC_REC
CSFB_FBS
CSFB_FRE
CSFB_REC
CSFA_REC
CSFA_FBS
CSFA_FRE
B
CSF A
Gene expression of CSF-A FBS samples
Gene expression of CSF-A FRE samples
R = 1, p < 2.2e-16
Gene expression of CSF-A REC samples
Gene expression of CSF-A FRE samples
R = 1, p < 2.2e-16
CSF B
Gene expression of CSF-B FBS samples
Gene expression of CSF-B FRE samples
R = 0.98, p < 2.2e-16
Gene expression of CSF-B REC samples
Gene expression of CSF-B FRE samples
R = 0.98, p < 2.2e-16
CSF C
Gene expression of CSF-C FBS samples
Gene expression of CSF-C FRE samples
R = 0.94, p < 2.2e-16
Gene expression of CSF-C REC samples
Gene expression of CSF-C FRE samples
R = 1, p < 2.2e-16

Figure 3

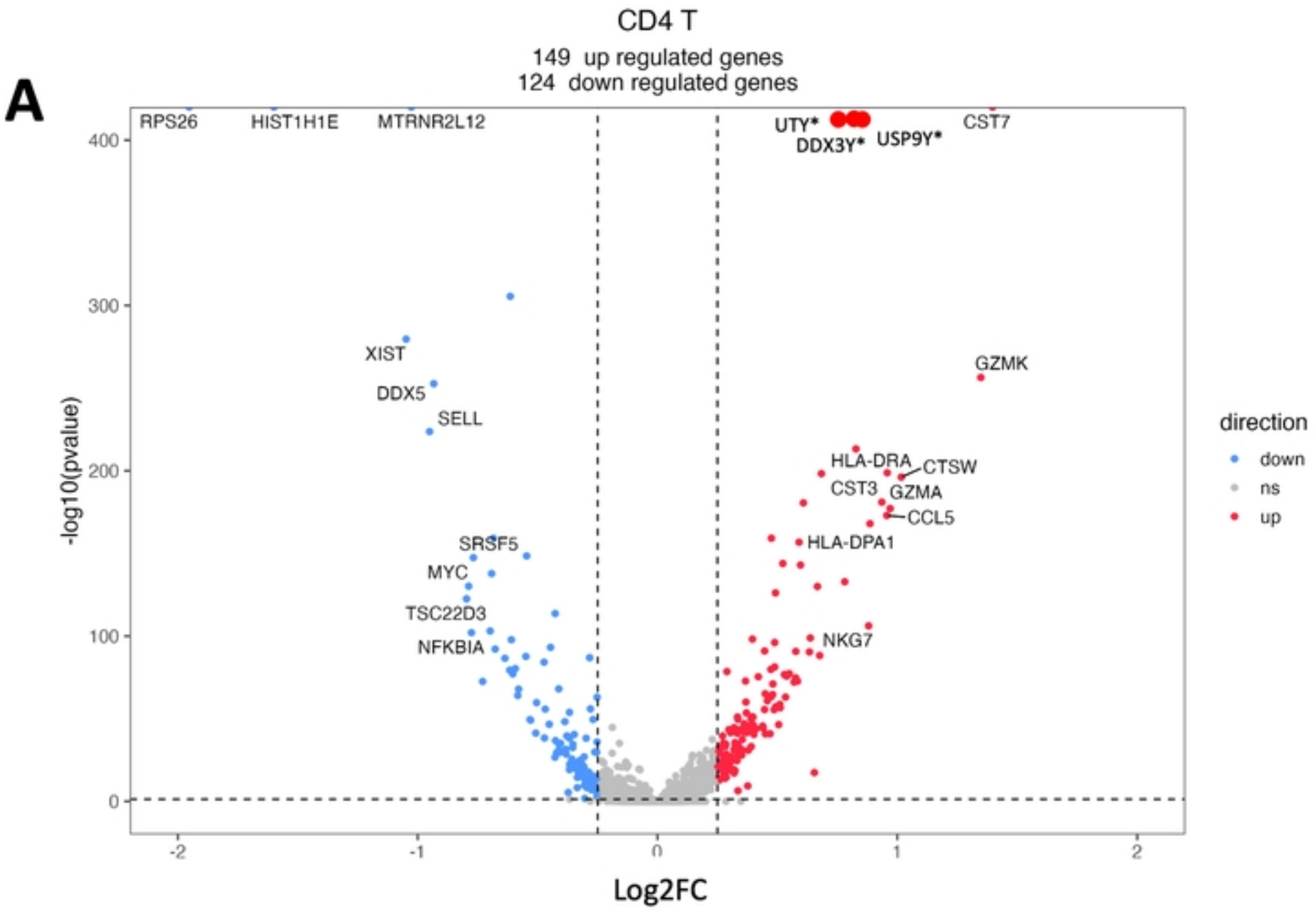
A
CD4 T
149 up regulated genes
124 down regulated genes
RPS26
HIST1H1E
MTRNR2L12
UTY*
DDX3Y*
USP9Y*
CST7
XIST
DDX5
SELL
GZMK
HLA-DRA
CTSW
CST3
GZMA
CCL5
HLA-DPA1
SRSF5
MYC
TSC22D3
NFKBIA
NKG7
-log10(pvalue)
Log2FC
direction
down
ns
up

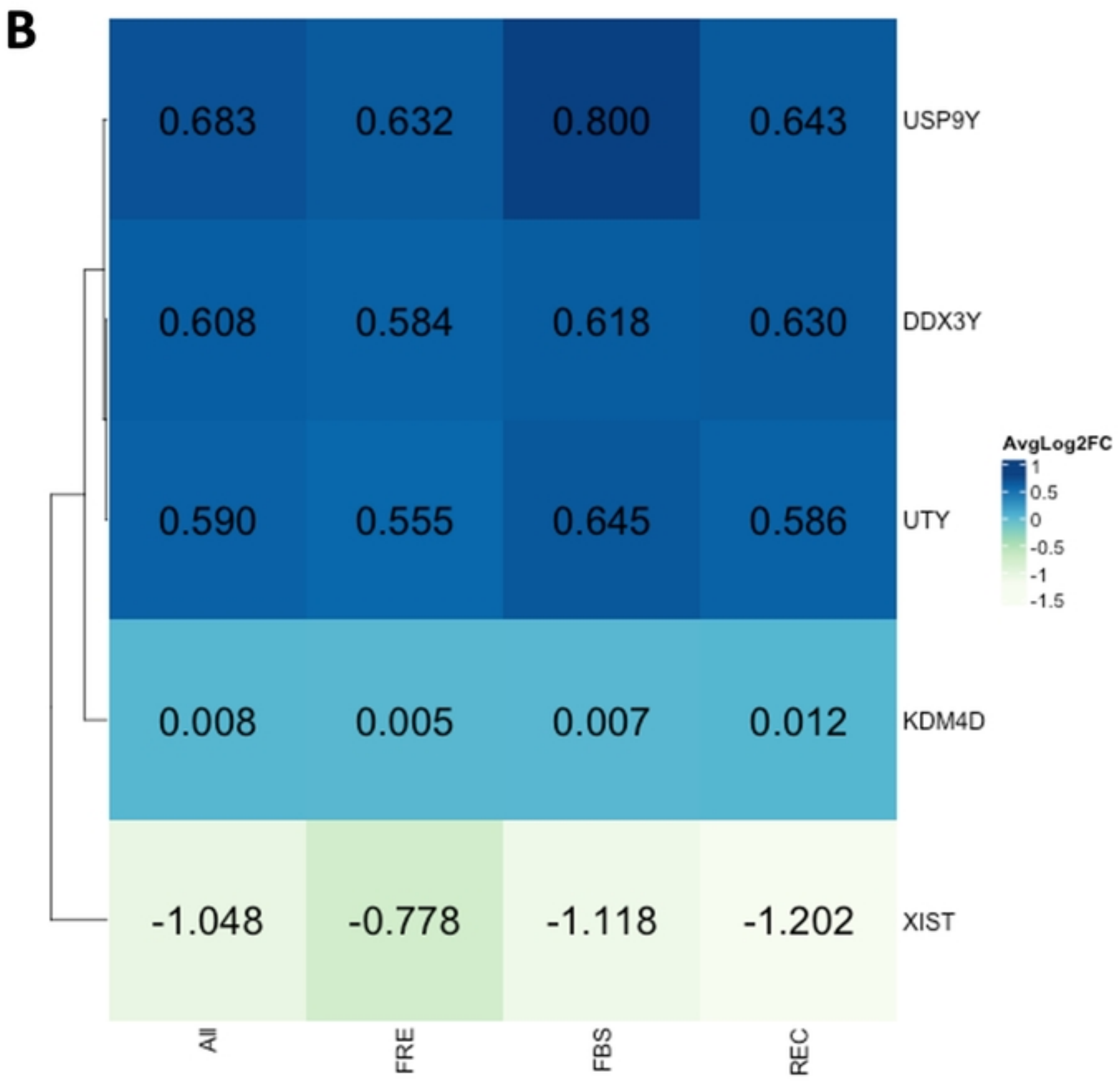
B
0.683
0.632
0.800
0.643
USP9Y
0.608
0.584
0.618
0.630
DDX3Y
0.590
0.555
0.645
0.586
UTY
0.008
0.005
0.007
0.012
KDM4D
-1.048
-0.778
-1.118
-1.202
XIST
All
FRE
FBS
REC
AvgLog2FC

Figure 4